HOSTED BY
ELSEVIER

Available online at www.sciencedirect.com
ScienceDirect

ICT Express ▮ (▮▮▮▮) ▮▮▮–▮▮▮

www.elsevier.com/locate/icte

Sum rates of asynchronous GFDMA and SC-FDMA for 5G uplink

Woojin Park, Hyun Jong Yang*, Hyunmyung Oh

School of Electrical and Computer Engineering, UNIST, Ulsan 689-798, Republic of Korea

Received 15 September 2015; received in revised form 30 November 2015; accepted 16 December 2015

Abstract

The fifth generation (5G) of mobile communication envisions ultralow latency less than 1 ms for radio interface. To this end, frameless asynchronous multiple access may be needed to allow users to transmit instantly without waiting for the next frame start. In this paper, generalized frequency division multiple-access (GFDMA), one of the promising multiple-access candidates for 5G mobile, is compared with the conventional single-carrier FDMA (SC-FDMA) in terms of the uplink sum rate when both techniques are adapted for the asynchronous scenario. In particular, a waveform windowing technique is applied to both schemes to mitigate the inter-user interference due to non-zero out-of-band emission.

Keywords: GFDMA; SC-FDMA; Out-of-band (OOB) emision; Asynchronous; Uplink sum rate

1. Introduction

The fifth generation (5G) of mobile communication is expected to support futuristic wireless services such as augmented reality, streaming gaming, and remote surgery. Recently, 5G network consortiums and standard bodies, such as NGMN, 5G-PPP, and ITU-R, have agreed to define the radio-interface latency requirement for the 5G to be less than 1 ms to support real-time services [1].

In current cellular uplink technology, which features single-carrier frequency division multiple-access (SC-FDMA) [2], all users must be frame-synchronized before transmission. The minimum transmission time interval (TTI) defined in the LTE is 1 ms, which would be the lowest fundamental limit on the latency for 5G. In practice, however, the uplink latency is much longer than 1 ms, because resource allocation and user scheduling require additional time.

In this context, much effort and attention have been paid to asynchronous multiple-access techniques in pursuit of removing the fundamental latency limit in the synchronous structure. For a modulating method to be employed in the asynchronous schemes, the transmit signal must show small out-of-band (OOB) leakage, thus yielding small intercarrier interference (ICI).

One of the candidates that meet this requirement is generalized frequency division multiplexing (GFDM) [3,4], which includes conventional orthogonal frequency division multiplexing (OFDM) [4] and single-carrier frequency division multiplexing (SC-FDM) as special cases [5]. The GFDM technique allows the spectrum shape to be tailored for low OOB emission. The OOB spectrum of GFDM was analyzed and compared with that of OFDM in the literature [4,6].

However, one may suggest the use of conventional SC-FDMA in an asynchronous manner for cellular uplink scenario. However, the spectrum of SC-FDMA is the same as the spectrum of OFDM [7], which has higher OOB emission than GFDM. Therefore, employing SC-FDMA asynchronously may generate high ICI among users owing to high OOB emission [2,8].

In this paper, the uplink sum rates of SC-FDMA and generalized frequency division multiple-access (GFDMA) are compared for both schemes are applied in the asynchronous scenario, which, to the best of the authors' knowledge, has not been explicitly published. Through numerical simulations, we have observed that determining the superior sum-rates between the two depends on the scenario, such as user density and signal-to-noise ratio (SNR).

* Corresponding author.
E-mail addresses: wjpark@unist.ac.kr (W. Park), hjyang@unist.ac.kr (H.J. Yang), ohhm1@unist.ac.kr (H. Oh).

Peer review under responsibility of The Korean Institute of Communications Information Sciences.

http://dx.doi.org/10.1016/j.icte.2015.12.002

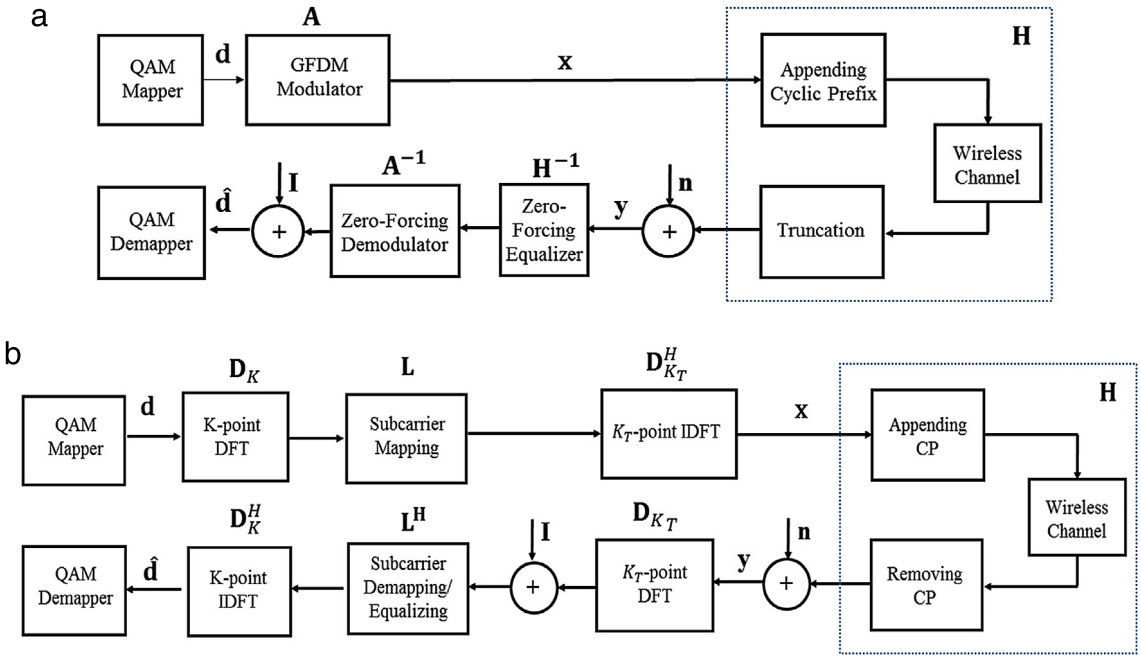

Fig. 1. Discrete-time representation of transceiver of (a) GFDMA and (b) SC-FDMA.

2. System model

2.1. Transceiver design in discrete-time representation

(1) *Discrete-time system model*: The $KM(=N)$-dimensional transmit signal vector is denoted by $\mathbf{x}$, where K is the number of subcarriers, and M is the number of sub-symbol blocks in GFDM [4]. In the case of SC-FDM, $M = 1$. The signal is added with a cyclic prefix (CP), passes through a discrete wireless channel, and is truncated to remove the CP in sequence. This process is equated as

$$\mathbf{y} = \mathbf{H}\mathbf{x} + \mathbf{n}, \tag{1}$$

where $\mathbf{H} \in \mathbb{C}^{N\times N}$ is the circular equivalent channel matrix, $\mathbf{y} \in \mathbb{C}^{N\times N}$ is the vector of the received signal in the discrete time domain, and $\mathbf{n}$ is the additive white Gaussian noise (AWGN) vector with size N whose elements all have zero mean and variance σ_0^2.

(2) *GFDMA*: The block diagram of GFDM transceivers is drawn in Fig. 1(a). The N-dimensional quadrature amplitude modulation (QAM) symbol vector is denoted by $\mathbf{d}$, and $(m \cdot K + k + 1)$th entry in $\mathbf{d}$ is represented by $d_{m,k}$ ($k \in \{0, \ldots, K-1\}$, $m \in \{0, \ldots, M-1\}$). The discrete-time transmit signal is then given by

$$x[n] = \sum_{k-0}^{K-1}\sum_{m-0}^{M-1}(g_{k,m}[n] \cdot d_{k,m}), \quad n = 0, \ldots, N \tag{2}$$

where $g_{k,m}[n] = g_{0,0}[(n - mK) \bmod N]$, and $g_{0,0}[n]$ is the discrete-time *GFDM* pulse shape for the first subcarrier and the first sub-symbol [4].

The transmit signal vector $\mathbf{x} = [x[0], x[1], \ldots, x[N-1]]^T$ is obtained from

$$\mathbf{x} = \mathbf{A}\mathbf{d}, \tag{3}$$

where $\mathbf{A}$ is the $(KM \times KM)$-dimensional signal generation matrix, defined as [4]

$$\mathbf{A} = (\mathbf{g}_{0,0} \quad \cdots \quad \mathbf{g}_{K-1,0} \quad \mathbf{g}_{0,1} \quad \cdots \quad \mathbf{g}_{K-1,M-1}). \tag{4}$$

Here $\mathbf{g}_{k,m} = \left[g_{k,m}[0], g_{k,m}[1], \ldots, g_{k,m}[N-1]\right]^T$, and $k \in \{0, 1, \ldots, K-1\}$, $m \in \{0, 1, \ldots, M-1\}$.

The zero-forcing method is applied to obtain the estimated QAM signal $\mathbf{d}'$ as

$$\mathbf{d}' = \mathbf{A}^{-1}\mathbf{H}^{-1}\mathbf{y} + \mathbf{I}, \tag{5}$$

where $\mathbf{I}$ is the ICI vector of size N, which will be discussed in Section 3.

(3) *SC-FDMA*: Given the same QAM symbol vector $\mathbf{d}$ as in GFDMA, the discrete-time transmit signal vector in SC-FDMA is obtained from [2,8]

$$\mathbf{x} = \mathbf{D}_{K_T}^H\mathbf{L}^H\mathbf{D}_K\mathbf{d}, \tag{6}$$

and the estimated QAM signal can be obtained as

$$\mathbf{d}' = \mathbf{D}_K^H\mathbf{L}^H(\mathbf{D}_{K_T}\mathbf{y} + \mathbf{I}), \tag{7}$$

where $\mathbf{D}_k \in \mathbb{C}^{k\times k}$ is discrete Fourier transform matrix, $\mathbf{L}$ is the reshaping matrix that transforms a vector from size K to K_T by zero-padding on unused subcarriers. Here, K_T is the total number of subcarriers on the entire multiple access system.

2.2. Power spectral density of SC-FDM and GFDM

(1) *PSD of SC-FDM*: The transmit signal in the continuous time domain by [8]

$$s(t) = \left(\sum_{k=0}^{K-1}[\mathbf{D}_K\mathbf{d}]_{k+1,1}e^{j2\pi\frac{k}{T_{fft}}t}\right) \cdot w(t), \tag{8}$$

Please cite this article in press as: W. Park, et al., Sum rates of asynchronous GFDMA and SC-FDMA for 5G uplink, ICT Express (2016), http://dx.doi.org/10.1016/j.icte.2015.12.002

Table 1
Windowing function shape in frequency domain.

	Time/frequency function
Without windowing	$W(f) = (T_{fft} + T_{CP})\text{sinc}((T_{fft} + T_{CP})f)e^{-j2\pi\Delta Tf}$
With windowing (ERC)	$W(f) = (T_{fft} + T_{CP} + T_w)\text{sinc}\left((T_{fft} + T_{CP} + T_w)f\right) * \left\{\frac{\cos(\pi T_w f)}{1-4T_w^2 f^2}\right\} e^{-j2\pi\Delta Tf}$

where T_{fft} is the time duration of a symbol, and $w(t)$ is the transmitter's windowing function. Here, $[\mathbf{X}]_{a,b}$ denotes the (a, b)th element of matrix $\mathbf{X}$. The non-windowed signal can also be represented by the windowing function whose shape is rectangular. The windowing function in the frequency domain are arranged in Table 1. In Table 1, '$*$' denotes the continuous convolution operation, T_{CP} is the time duration for CP, and T_w is the time expended in the case where windowing is applied. In case of non-windowed signals, T_w is set to be zero. The variable $\Delta T = (T_{fft} - T_{CP})/2$ denotes the offset from the start time of the data to the center of a window.

The power spectral density (PSD) of SC-FDM is derived by the same equation as in OFDM. From the Weinner–Kinchin theorem, PSD is derived as [7,9]

$$P_{\text{SC-FDM}}(f) = \frac{1}{T_b}\sum_{k=0}^{K-1}\left|W\left(f - \frac{k}{T_{fft}}\right)\right|^2, \tag{9}$$

where T_b is the total time duration of a symbol transmission and is equivalent to $T_{fft} + T_{CP} + T_w$.

(2) *PSD of GFDM*: Similar to the SC-FDM case, the windowed transmission signal can be given by [4]

$$s(t) = \left(\sum_{m=0}^{M-1}\sum_{k=0}^{K-1} d_{k,m}e^{j2\pi\frac{k}{T_{fft}}t}\cdot g(t - mT_{fft})\right)\cdot w(t), \tag{10}$$

where $g(t)$ is the continuous-time GFDM pulse shape and is defined as [4]

$$g(t) = \mathcal{F}^{-1}\left(\sum_{q=-\infty}^{\infty} G_{\text{filt}}\left(\frac{q}{MT_{fft}}\right)\delta\left(f - \frac{q}{MT_{fft}}\right)\right). \tag{11}$$

Here, the operator $\mathcal{F}^{-1}(G)$ represents the inverse Fourier transform of the spectrum G. The function $G_{\text{filt}}(f)$ in (11) is the normalized spectrum filter [4]. In this study, the RC filter with a roll-off factor $\alpha = 0.5$, is used.

$$G_{\text{filt}}(f) = \frac{1}{2}\left(1 - \cos\left(\pi\,\text{lin}_\alpha\left(\frac{f}{M}\right)\right)\right), \tag{12}$$

where $\text{lin}_\alpha(x) = \min[1, \max\{0, (1-\alpha)/2\alpha - |x|/\alpha\}]$.

Hence, the PSD is derived as [4,9]

$$P_{\text{GFDM}}(f) = \frac{1}{\left(MT_{fft}\right)^2 T_b'}\sum_{k=0}^{K-1}\sum_{m=0}^{M-1}\left|\sum_{p=-M}^{M} G_{filt}\left(\frac{p}{MT_{fft}}\right)\right.$$
$$\left.\times W\left(f - \frac{p}{MT_{fft}} - \frac{k}{T_{fft}}\right)e^{-j2\pi\frac{m}{M}p}\right|^2 \tag{13}$$

where T_b' is the total time duration of the symbol transmission in GFDM, given by $MT_{fft} + T_{CP} + T_w$. Note that T_b' is different from T_b.

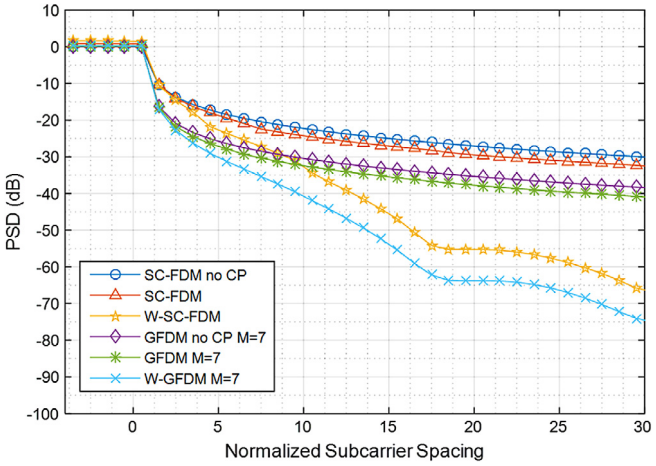

Fig. 2. PSD for SC-FDM and GFDM with and without waveform windowing.

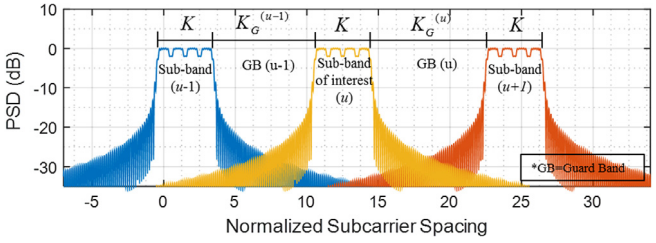

Fig. 3. PSD in GFDMA for $M = 7$ and $K = 4$.

Fig. 2 illustrates the PSD versus normalized subcarrier spacing on SC-FDM and GFDM with two windowing functions in Table 1. The windowed signals, prefixed with W-, show relatively lower OOB spectra than their corresponding non-windowed signals, especially with a large guard band. Comparing SC-FDM and GFDM, it is found that GFDM shows lower OOB spectra emission for all intervals.

3. Sum rate calculation

In this paper, N_U users occupy sub-bands consisting of K subcarriers out of K_T total subcarriers. Between two neighboring sub-bands, a guard band is inserted as depicted in Fig. 3.

Because two adjacent sub-bands are the most dominant sources of ICI, the OOB spectra emissions from the other users are ignored aside from these two. Therefore, the PSD of interfering signals at the kth subcarrier on user u is calculated as

$$\rho^{(u,k)} = P_{tr}P\left(\frac{K + K_G^{(u-1)} + k}{T_{fft}}\right)$$

Please cite this article in press as: W. Park, et al., Sum rates of asynchronous GFDMA and SC-FDMA for 5G uplink, ICT Express (2016), http://dx.doi.org/10.1016/j.icte.2015.12.002

$$+ P_{tr} P\left(\frac{2K + K_G^{(u)} - (k+1)}{T_{fft}}\right),$$
$$k \in \{0, 1, \ldots, K-1\},\ u \in \{2, 3, \ldots, N_U - 1\}, \quad (14)$$

where P_{tr} is the transmit power per subcarrier, and $K_G^{(u)}$ is the number of guard subcarriers between the uth and $(u+1)$th sub-bands. The function '$P(f)$' in (14) is one of the PSD functions: $P_{\text{SC-FDM}}(f)$ or $P_{\text{GFDM}}(f)$. In addition, if a user is on the lowest- or highest-frequency sub-band—i.e., $u = 1$ or $u = N_U$, the first or second term in (14) is deleted, respectively.

The N-element vector of ICI on the user u, $\mathbf{I}^{(u)}$, can be modeled by assuming that elements are independent Gaussian random variables. The $(mK + k + 1)$th element in $\mathbf{I}^{(u)}$ has zero mean and variance value $\rho^{(u,k)}$, where $k \in \{0, \ldots, K-1\}$, $m \in \{0, \ldots, M-1\}$.

3.1. Sum rate on asynchronous SC-FDMA

From the result in [8] on the derivation of the sum rate for SC-FDMA based on minimum mean-square error demodulation under an AWGN channel environment, the noise term on the frequency domain can be replaced by an interference-plus-noise term, whose variance is the sum of two variances of the noise and ICI terms. Therefore, the sum rate is derived as

$$R_{\text{SC-FDMA}} = \frac{N_U}{T_b} \log\left(1 + \left(\frac{1}{\frac{1}{K}\sum_{k=0}^{K-1} \frac{P_{tr}}{P_{tr}+\sigma_0^2+\rho^{(u,k)}}} - 1\right)^{-1}\right). \quad (15)$$

3.2. Sum rate on asynchronous GFDMA

As in SC-FDMA, the sum rate of the GFDMA based on zero-forcing demodulation in AWGN channel is derived by replacing the noise term with the interference plus noise term as

$$R_{\text{GFDMA}} = \frac{N_U}{T_b'} \sum_{m=0}^{M-1} \sum_{k=0}^{K-1} \log\left(1 + \frac{P_{tr}}{\sigma_0^2 [\mathbf{A}^{-1}\mathbf{A}^{-H}]_{i,i} + \rho^{(u,k)}}\right) \quad (16)$$

where $i = mK + k + 1, k \in \{0, \ldots, K-1\}$, and $m \in \{0, \ldots, M-1\}$.

4. Numerical results

4.1. Simulation parameters

The system parameters considered in the simulations are summarized in Table 2. In addition, the number of subcarriers per guard band, $K_G^{(u)}$, is calculated as

$$K_G = \left\lfloor \frac{K_T - K N_U}{N_U - 1} \right\rfloor \quad (17)$$

where $\lfloor a \rfloor$ represents the largest integer that is smaller or equal to a.

Table 2
System parameters.

Parameter	Value
T_{fft}	66.7 μs
T_{CP}	4.7 μs
T_w	4.7 μs
K_T	100
Subcarrier spacing	15 kHz
Bandwidth	1.5 MHz

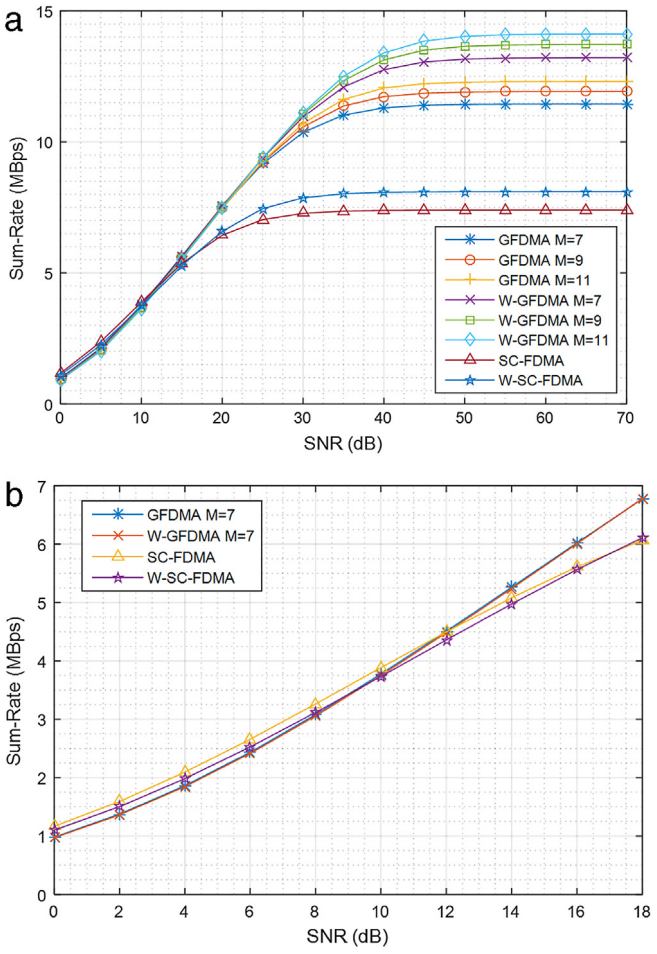

Fig. 4. Sum rates vs. SNR for $K = 12$, $K_G = 2$, $N_U = 6$ for SNR of (a) 0–70 and (b) 0–18 dB.

4.2. Sum rate vs. signal-to-noise ratio

Fig. 4(a) shows the sum rates versus SNR for $K = 12$, $K_G = 2$, and $N_U = 6$. It is seen that in the high SNR regime with values higher than 30 dB, where the ICI due to non-zero OOB emissions from other users is dominant to noise, the family of GFDMA techniques exhibit higher sum rates than the SC-FDMA techniques. The windowing technique provides a marginal sum rate gain for both SC-FDMA and GFDMA. As M increases in GFDMA, the sum rate increases owing to the reduced portion of CP duration and reduced OOB emission.

Fig. 4(b) shows the same results as in Fig. 4(a) but is enlarged for the practical SNR range of 0–18 dB. It is seen that for the low to intermediate SNR regime—i.e., 0–12 dB, where

Please cite this article in press as: W. Park, et al., Sum rates of asynchronous GFDMA and SC-FDMA for 5G uplink, ICT Express (2016), http://dx.doi.org/10.1016/j.icte.2015.12.002

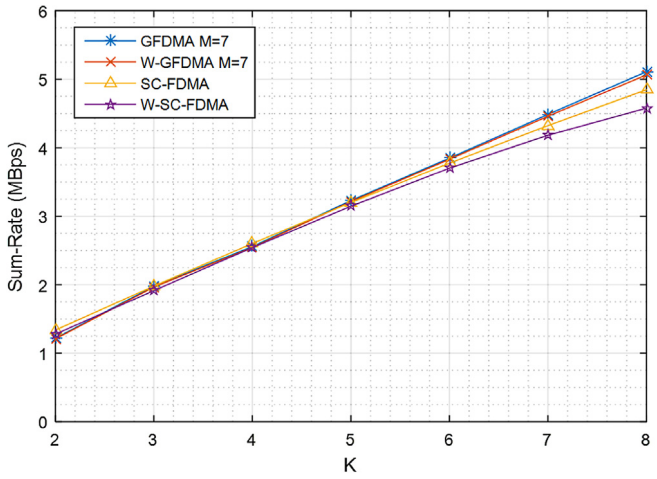

Fig. 5. Sum rates vs. K for SNR $= 12$ dB and $N_U = 12$.

the noise is dominant, SC-FDMA shows the highest sum rate. However, beyond 12 dB of SNR, where the ICI is dominant, the GFMD techniques show better sum rates than the SC-FDMA techniques.

4.3. Sum rate vs. subcarrier per user

Fig. 5 shows the sum rates vs. K for SNR $= 12$ dB and $N_U = 12$. For small K, from 2 to 4, the number of guard subcarriers is large, and thus there is enough space in the frequency domain to avoid OOB emission from neighboring sub-bands. However, as K increases by more than 4, where frequency spectrum utilization efficiency is high, the number of guard band subcarriers becomes small, and hence the GFDM exhibits higher sum rates.

5. Conclusion

In this paper, the PSD and uplink sum rate of SC-FDMA and GFDMA with windowing have been compared in the AWGN channel. Owing to low OOB emission in the GFDM PSD, the uplink sum rate of GFDMA becomes higher than that of SC-FDMA in the scenario where the number of guard band subcarriers is small—i.e., high user density with $K > 4$—or where the SNR is higher than 15 dB—i.e., ICI dominates noise.

Apart from the sum rate, the peak-to-average-power ratio in GFDM, which is an also important performance measure in the uplink, can be reduced significantly as in SC-FDM by employing the DFT spreading technique [5].

Acknowledgment

This work was supported by an IITP grant funded by the Korea government (MSIP) (No. B0126-15-1064, Research on Near-Zero Latency Network for 5G Immersive Service).

References

[1] IMT Vision, Framework and overall objectives of the future development of IMT for 2020 and beyond, ITU, HCMC, Viet Nam, February 2014.
[2] H.G. Myung, J. Lim, D.J. Goodman, Single-carrier FDMA for uplink wireless transmission, IEEE Veh. Technol. Mag. 1 (3) (2006) 30–38.
[3] G. Fettweis, M. Krondorf, S. Bittner, GFDM-generalized frequency division multiplexing, in: Proc. IEEE Veh. Tech. Conf., Barcelona, Spain, 2009.
[4] N. Michailow, M. Matthe, I.S. Gaspar, A.N. Caldevilla, L.L. Mendes, A. Festag, G. Fettweis, Generalized frequency division multiplexing for 5th generation cellular networks, IEEE Trans. Commun. 62 (9) (2014) 3045–3061.
[5] S.S. Das, S. Tiwari, Discrete Fourier transform spreading-based generalized frequency division multiplexing, Electron. Lett. 51 (10) (2015) 789–791.
[6] M. Matthe, Influence of pulse shaping on bit error rate performance and out of band radiation of generalized frequency division multiplexing, in: Proc. IEEE Int'l Conf. Commun., Sydney, Australia, 2014.
[7] H. Jung, M. Cudak, K. Baum, V. Nangia, Out-of-band emission of OFDM and SC-FDMA, in: IEEE 802.16 Broadband Wireless Access Working Group, March 2008.
[8] H.G. Myung, D.J. Goodman, Single Carrier FDMA: A New Air Interface for Long Term Evolution, Wiley, New York, 2008.
[9] J.A. Gubner, The Wiener–Kinchin theorem, in: Probability and Random Processes for Electrical and Computer Engineers, Cambridge Univ. Press, New York, 2006, pp. 421–423.

Please cite this article in press as: W. Park, et al., Sum rates of asynchronous GFDMA and SC-FDMA for 5G uplink, ICT Express (2016), http://dx.doi.org/10.1016/j.icte.2015.12.002